Nuclear Instruments and Methods in Physics Research B 267 (2009) 330–333

Contents lists available at ScienceDirect

Nuclear Instruments and Methods in Physics Research B

journal homepage: www.elsevier.com/locate/nimb

Carrier-envelope phase dependence in atomic ionization by short-laser pulses

D.G. Arbó [a,b,*], E. Persson [b], K.I. Dimitriou [c,d], J. Burgdörfer [b]

[a] Institute for Astronomy and Space Physics, IAFE, CC 67, Suc. 28 (1428) Buenos Aires, Argentina
[b] Institute for Theoretical Physics, Vienna University of Technology, Vienna, Austria
[c] Physics Department, National Technical University, Athens, Greece
[d] Theoretical and Physical Chemistry Institute, National Hellenic Research Foundation, Athens, Greece

ARTICLE INFO

Available online 22 October 2008

PACS:
32.80.Rm
32.80.Fb
03.65.Sq

Keywords:
Carrier-envelope phase
Short-laser pulse
Angular momentum

ABSTRACT

In atomic ionization by few-cycle laser pulses doubly differential momentum distributions near-threshold exhibit a radial nodal structure that results from peaked partial-wave distributions near a particular angular momentum. We analyze the doubly differential momentum distribution for different carrier-envelope phases. We find that in the cases where the photoelectron reaches a minimum at threshold the angular momentum distribution is very sensitive to the CEP since small variations of the ponderomotive energy can lead to the opening or closing of a new channel.

© 2008 Elsevier B.V. All rights reserved.

1. Introduction

The interaction of few-cycle pulses with matter has attracted considerable interest as shorter laser pulses have become available. Ultrashort pulses for which the pulse length τ becomes comparable to the optical period T lead to novel features of laser–matter interactions, among them are the strong carrier-envelope phase (CEP) dependence of excitation and ionization processes [1–3]. Rudenko et al. [4] and Maharjan et al. [5] presented fully two-dimensional momentum maps for laser-ionized electrons for different rare gases. The near-threshold structures observed have recently been semiclassically explained in terms of a classical angular momentum distribution sharply peaked [6,7] near the quantum number l_0. Such distributions in the near-threshold continuum result from the interplay between the laser and the Coulomb fields [8,9]. The existence of subpeaks in the photoelectron spectra of rare-gas atoms was explained by the rapidly changing ponderomotive potential in the short laser pulse [10]. The effect of channel closing on the photoionization yield has been extensively studied [11–13].

In the present work we study the CEP-dependence of the momentum distributions of ejected electrons. We show that the dominant angular momentum distribution near-threshold is sensitive to variations in the CEP in the case that a new channel appears, that is, when there is a minimum of the photoelectron spectrum very close to threshold. Here, the CEP-dependence of the ponderomotive energy leads to a CEP-dependence of the doubly differential momentum distributions. Atomic units are used throughout.

2. Carrier-envelope phase dependent ponderomotive energy

We consider an atom interacting with a linearly polarized laser field. Within the single active electron approximation the Hamiltonian is

$$H = \frac{\vec{p}^2}{2} + V(r) + \vec{r}\cdot\vec{F}(t), \tag{1}$$

where $\vec{p}$ and $\vec{r}$ are the momentum and position of the electron, respectively, $V(r)$ is the atomic central potential, and $\vec{F}(t)$ is the time dependent external field, which we choose as

$$\vec{F}(t) = F_0 \cos^2\left(\frac{\pi t}{\tau}\right)\cos(\omega t + \varphi_{CE})\hat{z}; \quad -\tau/2 \leqslant t \leqslant \tau/2, \tag{2}$$

and zero elsewhere. In Eq. (2), ω is the laser carrier frequency, φ_{CE} is the carrier-envelope phase, τ is the total pulse duration, F_0 is the peak field and $\hat{z}$ is the polarization direction.

The maximum field F_{max} reached according to Eq. (2) depends on the CEP for short pulses. For a cosine pulse, i.e. $\varphi_{CE} = 0$, the value of F_{max} coincides with the peak field F_0 while for any other value of the CEP $F_{max} < F_0$. We define a CEP-dependent ponderomotive energy related to the field maximum of the pulse as

$$U_p(\varphi_{CE}) = \frac{[F_{max}(\varphi_{CE})]^2}{4\omega^2}. \tag{3}$$

* Corresponding author.
E-mail address: diego@iafe.uba.ar (D.G. Arbó).

0168-583X/$ - see front matter © 2008 Elsevier B.V. All rights reserved.
doi:10.1016/j.nimb.2008.10.044

The value of the CEP-dependent ponderomotive energy $U_p(\varphi_{CE})$ agrees with the usual definition of the ponderomotive energy $U_p = (F_0/2\omega)^2$ only when $\varphi_{CE} = 0$. For other values of the CEP, the ponderomotive energy is reduced, i.e. $U_p(\varphi_{CE}) \leqslant U_p$. The maximum departure of $U_p(\varphi_{CE})$ from the value $U_p(0)$ occurs for sine-like pulses ($\varphi_{CE} = \pi/2$). The magnitude of the difference of the ponderomotive energy between a sine-like and a cosine-like peak ΔU_p is

$$\Delta U_p = U_p(0) - U_p(\pi/2). \tag{4}$$

Below we will analyze how the variation of $U_p(\varphi_{CE})$ affects the dominant angular momentum and the doubly differential momentum distribution near-threshold.

3. Quantum and classical electron dynamics

Angular momentum distribution have been explained by two different ionization mechanisms: (i) A biased random walk model assuming stochastic uncorrelated multiphoton processes [14] and (ii) a quasiclassical tunneling ionization process [7] calculated using classical-trajectory Monte-Carlo [15] simulations which incorporate tunneling through the potential barrier (CTMC-T). In (i), l_0 can be viewed as the most probable value after a biased random walk in momentum space assuming a stochastic uncorrelated multiphoton process: one electron with orbital quantum number l can absorb a photon and consequently undergoes a transition $l \to l+1$ with a probability p_+ or a transition $l \to l-1$ with a probability p_-, according to the dipole coupling.

In order to numerically solve the time dependent Schrödinger equation (TDSE) we employ the generalized pseudo-spectral method [16]. The calculation of the 2D momentum distribution requires projection of the wave function $|\psi(\tau/2)\rangle$ after the conclusion of the pulse onto outgoing continuum functions,

$$\frac{dP}{d\vec{k}} = \frac{1}{4\pi k}\left|\sum_l e^{i\delta_l(k)}\sqrt{2l+1}P_l(\cos\theta)\langle k,l|\psi(\tau/2)\rangle\right|^2. \tag{5}$$

Here $\delta_l(k)$ is the momentum-dependent atomic phase shift, θ is the angle between $\vec{k}$ and the polarization direction $\hat{z}$ of the laser field, P_l is the Legendre polynomial of degree l and $|\,k,l\rangle$ is the eigenstate of the free atomic Hamiltonian with positive eigenenergy $E = k^2/2$ and orbital quantum number l. For a rare-gas atom the atomic potential can be modeled as the sum of the asymptotic Coulomb potential plus a short-range potential that accounts for the departure from the pure coulombic behavior near the nucleus due to the screening by the other electrons [17]. In this case the atomic phase shift is the sum of the Coulomb phase shift and the phase shift due to the short-range potential [18], i.e. $\delta_l(k) = \delta_l^C(k) + \delta_l^{SR}(k)$. The latter was calculated numerically. The atom is assumed to be initially in its ground state. Due to the cylindrical symmetry for a linearly polarized laser field the magnetic quantum number remains conserved.

In Fig. 1 we show the angular distribution of the electron resulting from ionization of argon by a pulse of carrier frequency $\omega = 0.057$, peak field $F_0 = 0.065$, duration $\tau = 882$ and $\varphi_{CE} = 0$. We have projected the state at the end of the pulse onto the outgoing waves by using the atomic phase shift $\delta_l(k)$ and compare the results when only the Coulomb phase shift $\delta_l^C(k)$ is used. Some differences are observed indicating that the short-range core potential has a modest influence on the angular distribution. However, the overall structure is maintained i.e. the number of minima are the same. This is expected when the number of minima is controlled by a single angular momentum quantum number l_0, which is given directly by the partial-wave content at the end of the pulse without forming the coherent superposition (Eq. (5)).

A classical-trajectory Monte-Carlo method including tunnel effect (CTMC-T) [15,19,20] is employed to delineate the classical properties of the ionization. The CTMC-T method excludes, because

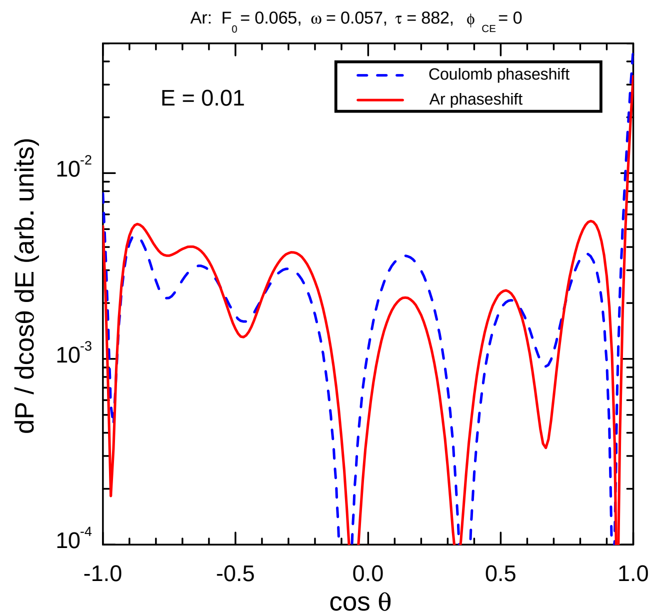

Fig. 1. Angular distribution of ejected electrons with energy $E = 0.01$ in ionization of argon by a laser of peak field $F_0 = 0.065$, frequency $\omega = 0.057$, pulse duration $\tau = 882$ and CEP $\phi_{CEP} = 0$. Dashed (blue) line corresponds to calculations performed with the Coulomb phase shift δ_l^C and solid (red) line corresponds to calculations performed with the full atomic phase shift δ_l. (For interpretation of the references in color in this figure legend, the reader is referred to the web version of this article.)

of its classical nature, any true multiphoton absorption process. The electron is allowed to tunnel through the potential barrier whenever it reaches the outer turning point, with a tunneling probability given by the WKB approximation. A typical electron trajectory after tunneling shows a quiver motion along the polarization of the laser field superimposed on a drift motion following an approximate Kepler hyperbola with the same final angular momentum [7]. As the angular momentum of the Kepler hyperbola is identical to that of the asymptotic angular momentum L of the laser-driven electron, we can identify the pericenter of the hyperbola with the quiver amplitude, $\alpha = (\sqrt{Z_T^2 + (kL)^2} - Z_T)/k^2$ with $\alpha = F_0/\omega^2$ and Z_T the asymptotic charge of the atomic potential,

$$L_0 = L(0) = (2Z_T\alpha)^{1/2}. \tag{6}$$

Two limitations should be emphasized: firstly, the classical expression does not consider dipole selection rules that may favor even or odd l_0; and secondly, L_0 is a real number while l_0 is integer. Consequently, such semiclassical estimates have an intrinsic error of $l_0 \pm 1$.

4. Results

In Fig. 2 we show the two-dimensional momentum distribution $\frac{d^2P}{dk_\rho dk_z} = 2\pi k_\rho\left(\frac{dP}{d\vec{k}}\right)$ for photoionization of atomic hydrogen by a laser pulse of peak field $F_0 = 0.075$, frequency $\omega = 0.05$ and total duration $\tau = 1005$, which comprises eight cycles. In Fig. 2(a) and (b) a cosine-like ($\varphi_{CE} = 0$) and a sine-like pulse ($\varphi_{CE} = \pi/2$) are used, respectively. Both frames in Fig. 2 display complex interference patterns characterized by a transition from a ring-shaped pattern at larger k with circular nodal lines to pronounced radial nodal lines near-threshold resembling experimental results [4,5].

Differences between the photoionization due to cosine- and sine-like pulses are clearly observed near-threshold. While the first ring in Fig. 2(a) extends up to $k = 0.27$ ($E = 0.036$), in Fig. 2(b) a small ring reaches $k = 0.15$ ($E = 0.011$). In this case, the difference of the ponderomotive energy between a cosine- and sine-like pulse is, accord-

Download English Version:

https://daneshyari.com/en/article/1682722

Download Persian Version:

https://daneshyari.com/article/1682722

Daneshyari.com